Preprints of the 21st IFAC World Congress (Virtual)
Berlin, Germany, July 12-17, 2020

Prescribed–time tracking for triangular systems of reaction–diffusion PDEs

Drew Steeves * **Leobardo Camacho-Solorio** * **Mouhacine Benosman** ** **Miroslav Krstic** *

* *Department of Mechanical & Aerospace Engineering, University of California, San Diego, CA (e-mails: {dsteeves, lcamacho, krstic}@ucsd.edu)*
** *Mitsubishi Electric Research Lab, Cambridge, MA (e-mail: benosman@merl.com)*

Abstract: Approximate controllability of systems of coupled parabolic partial differential equations has been of interest for a few decades, where the existence of open–loop control laws performing approximate state transitions within a finite time is studied. In this work, we specialize to systems of reaction–diffusion equations where the connectivity structure is triangular in the reaction parameters and the controls appear at the boundary. We first generate controllers by combining a decoupling backstepping approach with differential flatness that allow us to generate admissible trajectories for system outputs from a given initial condition. As a byproduct of our approach, we achieve approximate state transitioning for the system within a finite *terminal* time. We enhance our control law by introducing time–varying error feedback controllers which reject variations in initial conditions within the terminal time. The resulting control law not only performs the approximate control task but also output trajectory tracking, all within the terminal time which can be prescribed independently of initial conditions.

Keywords: Distributed–parameter systems, linear systems, trajectory planning, closed–loop systems, controllability.

1. INTRODUCTION

Controllability of systems of parabolic partial differential equations (PDEs) has been of interest to the mathematical controls community for some time (see, for example, Fattorini [1966], Fattorini and Russell [1971], Fursikov and Imanuvilov [1995]). A subset of these problems demand establishing the existence of open–loop control laws which perform *approximate* state transitions from a given initial condition to a desired terminal profile, within a finite terminal time. In these problems, the actuation typically appears in–domain or at the boundary; it was shown in [Ammar-Khodja et al., 2011, Thm. 2.2] that for a single equation, these actuation locations are interchangeable *for open–loop control laws*.

The interest in approximate controllability of systems of coupled parabolic PDEs stems from their utility in representing various physical behaviors: for example, they accurately model predator–prey populations Hastings [1978] and chemical processes involving reagents Winkin et al. [2000]. The ability to control these behaviors in desired ways has tangible engineering impacts. In these and many other applications, boundary control is the most feasible location of actuation.

While existential control problems are theoretically significant, *generating* the associated open–loop control laws is equally crucial in the realm of engineering. One method to produce these controllers is to exploit, if possible, a differential flatness property of the system, which was first developed for finite–dimensional systems Fliess et al. [1995] and later on advanced for PDEs Laroche et al. [2000]. For a single equation, the authors of Martin et al. [2014] demonstrate null (and hence approximate, see [Coron, 2007, Thm. 2.45]) controllability of the heat equation by exploiting differential flatness, satisfyingly linking theory and engineering applicability. However, for systems of PDEs, approaches relying on differential flatness are limited due to the severe constraints imposed by them.

Moreover, these open–loop control laws achieving approximate state transitioning along an output reference trajectory are valid for a single known initial condition – the one for which they were designed. This renders the ensuing controllers of little use in most applications where initial conditions vary, requiring a computationally–expensive recalculation of the open–loop control laws. To correct this shortcoming, [Krstic and Smyshlyaev, 2008, Sec. 12.2] employs error feedback at the boundary to drive the output to the reference trajectory. The resulting control law, developed using the backstepping approach, *exponentially* stabilizes the output to the reference trajectory. While this is satisfactory for many applications, others possessing strict time constraints require the state to converge to the reference trajectory within the terminal time, achieving the desired approximate state transition and output trajectory regardless of initial condition.

In the literature, related problems involving motion planning for *single* reaction–advection–diffusion equations Laroche et al. [2000], Meurer [2012] and exponential stabilization of coupled parabolic systems by means of boundary feedback Baccoli et al. [2015], Vazquez and Krstic [2017], Camacho-Solorio et al. [2017] have been studied. More recently, finite–time stabilization of a single reaction–(advection)–diffusion equation Coron and Nguyen [2017], Espitia et al. [2019], Steeves et al. [2019] (or systems with equi–diffusivity, limiting its applicability) has been achieved. In these works, the time by which attractivity to the origin occurs can be prescribed independently of the initial conditions, herein referred to as *prescribed*–time stabilization.

This is the appropriate type of finite–time stabilization for this application (see Polyakov et al. [2015] for others). In this work, we rely on methodologies related to those developed in each of the three areas of motion planning, coupled system (exponential) stabilization, and prescribed–time stabilization for parabolic PDEs.

1.1 Contributions

Our contributions are twofold. We first develop a control law that achieves desired approximate (possibly *non–stationary*) state transitioning (in the sense of approximate controllability, see [Coron, 2007, Def. 2.40] for details) or assignment of an admissible output trajectory for a *system* of reaction–diffusion equations, where the triangular connectivity structure appears as reactivity–type cascading. We achieve this by first developing a feedback controller via the backstepping approach that effectively decouples the equations using a treatment similar to Camacho-Solorio et al. [2017] (it eliminates the reaction terms), followed by an approach which leverages differential flatness of the resulting decoupled heat equations to perform the state transitioning and trajectory assignment task via an open–loop controller. Our second contribution enhances the first by supplementing the control law with time–varying error feedback which performs the task of *prescribed*–time trajectory tracking for different initial conditions than those used to design the open–loop controller. This feedback relies on the time–varying backstepping methodology developed in Steeves et al. [2019].

2. PROBLEM STATEMENT

Consider the linear reaction–diffusion system given by

$$\frac{\partial u}{\partial t}(x,t) = \Sigma \frac{\partial^2 u}{\partial x^2}(x,t) + \Lambda(x) u(x,t), \tag{1}$$

for $(t,x) \in (t_0, t_0+T) \times (0,1)$ with state

$$u(x,t) = [u_1(x,t), \ldots, u_n(x,t)]^T, \tag{2}$$

model parameters

$$\Sigma := \operatorname{diag}(\varepsilon_1, \ldots, \varepsilon_n) \in \mathbb{R}^{n\times n}, \tag{3}$$

$$\Lambda(x) := \begin{bmatrix} \lambda_{11}(x) & \lambda_{12}(x) & \cdots & \lambda_{1n}(x) \\ 0 & \lambda_{22}(x) & \ddots & \vdots \\ \vdots & \vdots & \ddots & \lambda_{n-1,1}(x) \\ 0 & 0 & \ldots & \lambda_{nn}(x) \end{bmatrix} \in \mathbb{R}^{n\times n}, \tag{4}$$

and boundary conditions

$$\frac{\partial u}{\partial x}(0,t) = [0, \ldots, 0]^T \in \mathbb{R}^n, \tag{5}$$

$$u(1,t) = U(t), \tag{6}$$

for $n \in \mathbb{N}_{\geq 2}$. We are concerned with the trajectory of the system output

$$y(t) = [y_1(t), \ldots, y_n(t)]^T := u(0,t) \in \mathbb{R}^n. \tag{7}$$

We denote by $u_0 \in \mathcal{L}^2([0,1];\mathbb{R}^n)$ the initial conditions of (1); we assume that $0 < \varepsilon_n < \varepsilon_{n-1} < \cdots < \varepsilon_1$ (for the equi–diffusivity case, one can adapt the treatment of Baccoli et al. [2015]). Due to the triangular structure of (4), this assumption restricts couplings to the equations with higher diffusivities. Our primary objective is to construct a boundary control law that achieves a state transition from $u_0(x)$ to a desired terminal profile, $u_T(x)$, along a desired admissible output trajectory and within the prescribed *terminal* time, T. Our secondary objective is to attenuate to zero error caused by uncertainty in the initial conditions within the terminal time.

2.1 Methodology

The boundary control (6) achieving the aforementioned objectives is constructed in three steps. First, a static feedback control law $U_{\mathrm{D}}[u(x,t)]$, $U_{\mathrm{D}}(t) \in \mathbb{R}^n$, is designed to *decouple* in a sense the couplings present in (1), that is, to eliminate the reaction matrix (4), rendering the system exponentially stable. This is achieved by using an invertible integral transformation T_{D} and a methodology similar to Camacho-Solorio et al. [2017]. Next, an open–loop control law $U_{\mathrm{T}}([u_0(x)])(t) \in \mathbb{R}^n$, $U_{\mathrm{T}}(t) \in \mathbb{R}^n$, is designed to perform approximate state transitions along a desired output trajectory. This is accomplished by exploiting differential flatness with respect to $y(t)$ with treatment similar to Laroche et al. [2000], Meurer [2012]. Lastly, time–varying error feedback $U_{\mathrm{PT}}[e(x,t)](t)$, $U_{\mathrm{PT}}(t) \in \mathbb{R}^n$, is developed to attenuate the error caused by variations in initial conditions to zero within the terminal time. This is attained by using an invertible time–varying integral transformation T_{PT} and utilizing damping methodologies similar to Steeves et al. [2019].

3. MAIN RESULT

We consider the problems of transitioning from any initial condition $u_0(x)$ of (1)–(6) to any desired terminal profile $u_T(x)$ at $t = t_0 + T$ and the tracking of the system output, $y(t)$, to a smooth trajectory $y_{\mathrm{ref}}(t) \in \mathbb{R}^n$ with $y_{\mathrm{ref}}(t_0) = u_0(0)$ and $y_{\mathrm{ref}}(t_0 + T) = u_T(0)$ (cf. (34)–(35) for details). We now present our main result concerning this problem, where we denote by $\mathbf{e}_i$ and $f^{(k)}(t)$ the ith canonical basis vector of $\mathbb{R}^n$ and the kth derivative of $f(t) \in C^k(\mathbb{R})$, respectively.

Theorem 1. For $u_0(x) \in \mathcal{L}^2(0,1)^n$ and $N \in \mathbb{N}$, the control law

$$\begin{aligned} U(t) = & \int_0^1 K_{\mathrm{D}}(1,z) u(z,t) dz + \sum_{i=1}^n \left(\sum_{k=0}^N \frac{y_{i,\mathrm{ref}}^{(k)}(t)}{\varepsilon_i^k (2k)!} \right) \mathbf{e}_i \\ & + \int_0^1 K_{\mathrm{PT}}(1,z,t-t_0) \Bigg[u(z,t) - \int_0^z K_{\mathrm{D}}(z,\xi) u(\xi,t) d\xi \\ & - \sum_{i=1}^n \left(\sum_{k=0}^N \frac{y_{i,\mathrm{ref}}^{(k)}(t) z^{2k}}{\varepsilon_i^k (2k)!} \right) \mathbf{e}_i \Bigg] dz, \end{aligned} \tag{8}$$

with K_{D} characterized in Lemma 3, K_{PT} given in (43) and y_{ref} selected in (34) drives the system from $u_0(x)$ to $\check{u}_T(x)$ such that, for any $\varepsilon := \varepsilon(N) > 0$,

$$\|\check{u}_T(\cdot) - u_T(\cdot)\|_{\mathcal{L}^2(0,1)^n} < \varepsilon \tag{9}$$

for N large enough, where $U(t)$ has smooth, time–varying control gains and remains bounded for all $t \in [t_0, t_0 + T)$. Moreover, $y(t) \in C^\infty([t_0, t_0 + T))$ and

$$y(t) - y_{\mathrm{ref}}(t) \to 0 \quad \text{as} \quad t \to t_0 + T, \tag{10}$$

that is, we achieve prescribed–time trajectory tracking of the output selected in (34).

The rest of this paper aims to establish Theorem 1.

3.1 Mapping to a decoupled system

Directly studying control and error stabilization of the system (1)–(6) creates difficulties in achieving open–loop trajectory tracking as well as prescribed–time error attenuation. We address this difficulty by first developing a boundary feedback controller which effectively cancels the reactivity matrix Λ, rendering the new system in decoupled form. We present this decoupling control law next.

Lemma 2. For $\mathcal{T} = \{(x,y) \in \mathbb{R}^2 \mid 0 \le y \le x \le 1\}$ and for the *kernel* function $K_D \in \mathcal{C}\left(\mathcal{T};\mathbb{R}^{2\times 2}\right)$ (cf. Lemma 3 for its characterization), consider the linear invertible transformation $T_D : \mathcal{L}^2\left([0,1];\mathbb{R}^2\right) \mapsto \mathcal{L}^2\left([0,1];\mathbb{R}^2\right)$ defined by

$$T_D[f(x)] = f(x) - \int_0^x K_D(x,y)f(y)dy, \tag{11}$$

with inverse

$$T_D^{-1}[f(x)] = f(x) - \int_0^x Q_D(x,y)f(y)dy. \tag{12}$$

By selecting the boundary feedback control $U(t) \in \mathbb{R}^2$ in (6) as

$$U(t) = \int_0^1 K_D(1,y)u(y,t)dy + U_T(t) + U_{PT}(t), \tag{13}$$

where U_T and U_{PT} are additional degrees of freedom utilized in Sections 3.2 and 3.3, (11) maps (1)–(6), into

$$\frac{\partial v}{\partial t}(x,t) = \Sigma\frac{\partial^2 v}{\partial x^2}(x,t), \tag{14}$$

$$\frac{\partial v}{\partial x}(0,t) = 0, \tag{15}$$

$$v(1,t) = U_T(t) + U_{PT}(t), \tag{16}$$

with $v(x,t) = T_D[u(x,t)]$ and initial condition

$$v_0(x) = (v_{0,1}(x),\ldots,v_{0,n}(x))^T = T_D[u_0(x)].$$

In addition, there exist finite $1 \le k_1, k_2 < \infty$ such that

$$\|v(\cdot,t)\|_{\mathcal{L}^2(0,1)^n} \le k_1\|u(\cdot,t)\|_{\mathcal{L}^2(0,1)^n}, \tag{17}$$

$$\|u(\cdot,t)\|_{\mathcal{L}^2(0,1)^n} \le k_2\|v(\cdot,t)\|_{\mathcal{L}^2(0,1)^n}, \tag{18}$$

Next, we present our study of the kernel function K_D.

Lemma 3. There exists a unique, continuous and piecewise–smooth $K_D \in \mathcal{C}\left(\mathcal{T};\mathbb{R}^{n\times n}\right)$ with components

$$K_D(x,y) = \begin{bmatrix} K_{D,11}(x,y) & K_{D,12}(x,y) & \cdots & K_{D,1n}(x,y) \\ 0 & K_{D,22}(x,y) & \ddots & \vdots \\ \vdots & \vdots & \ddots & K_{D,n-2,n}(x,y) \\ 0 & 0 & \cdots & K_{D,nn}(x,y) \end{bmatrix}, \tag{19}$$

satisfying

$$\Sigma\frac{\partial^2 K_D}{\partial x^2}(x,y) - \frac{\partial^2 K_D}{\partial y^2}(x,y)\Sigma = K_D(x,y)\Lambda, \tag{20}$$

for $(x,y) \in \mathcal{T}$, with boundary conditions

$$\Sigma K_D(x,x) - K_D(x,x)\Sigma = 0, \tag{21}$$

$$\frac{\partial K_D}{\partial y}(x,x)\Sigma + \Sigma\frac{\partial K_D}{\partial x}(x,x) + \Sigma\frac{d}{dx}[K_D(x,x)] = -\Lambda, \tag{22}$$

$$\frac{\partial K_D}{\partial y}(x,0) = 0, \tag{23}$$

$$K_D(0,0) = 0. \tag{24}$$

Due to limitations in space, the proofs of Lemmas 2 and 3 are not provided here, but follow similar arguments as in Camacho-Solorio et al. [2017]. We now pursue a open–loop control law which will ensure the desired state transitioning or output trajectory tracking for (14)–(16).

3.2 State transitioning and trajectory generation

In this section, we develop $U_T(t)$. We proceed as in Laroche et al. [2000] and rely on the differential flatness technique; one can obtain a more general treatment that allows for equations that include advection/reaction terms from Meurer [2012]. In this work, we focus on developing open–loop controllers for n heat equations. Moreover, since (14)–(16) is decoupled, it suffices to design the components of $U_T(t)$ separately, and hence it is adequate to study a single equation within (14)–(16). Consider the ith equation of (14)–(16), given by

$$\frac{\partial v_i}{\partial t}(x,t) = \varepsilon_i\frac{\partial^2 v_i}{\partial x^2}(x,t) \tag{25}$$

$$\frac{\partial v_i}{\partial x}(0,t) = 0, \tag{26}$$

$$v_i(1,t) = U_{T,i}(t) \tag{27}$$

for $i = 1,\ldots,n$, where $U_{T,i}(t)$ denotes the ith component of the open–loop controller. For the moment, take $U_{PT}(t) \equiv 0$. Notice that the *inverse equation* of (25)–(27) (that is, where spatial coordinates play the role of temporal ones and vice–versa, now with *initial conditions* $v_i(0,t)$ and $\frac{\partial v_i}{\partial x}(0,t)$) is in a form for which the Cauchy–Kowalevski theorem [Folland, 1995, Thm. 1.25] directly applies, provided that $v_i(0,t)$ and $\frac{\partial v_i}{\partial x}(0,t)$ are sufficiently regular near $t = t_0$. This regularity is ensured by generating a trajectory $y_i(t)$ with Gevrey class of order $s \in (1,2]$ (see Gevrey [1918] for a definition on Gevrey class; choosing $s = 1$ requires $y_i(t)$ to be analytic), due to (7), (11) and (26). Suppose for the moment that $y_i(t)$ is of the required regularity; then, we recover the (well–defined) solution to (25)–(27) of the form

$$v_i(x,t) = \sum_{k=0}^{\infty}\frac{v_i^k(t)x^k}{k!} \tag{28}$$

for smooth functions $\{v_i^k(t)\}_k \subset C^\infty(t_0, t_0+T)$. By substituting (28) into (25) and applying (7), (26)–(27), we obtain the characterizations

$$v_i(x,t) = \sum_{k=0}^{\infty}\frac{y_i^{(k)}(t)x^{2k}}{\varepsilon_i^k(2k)!} \tag{29}$$

and

$$U_{T,i}(t) = \sum_{k=0}^{\infty}\frac{y_i^{(k)}(t)}{\varepsilon_i^k(2k)!}, \tag{30}$$

where $y_i^{(k)}(t)$ denotes the kth derivative of the output. Hence, $y_i(t)$ is a *flat output* for (25)–(27). Given an initial condition $v_{0,i}(x) \in \mathcal{L}^2(0,1)$ and a desired terminal profile $v_{T,i}(x) \in \mathcal{L}^2(0,1)$, one can apply the Stone–Weierstrass theorem [Rudin et al., 1964, Thm. 7.32] to *uniformly* approximate these profiles by

$$\check{v}_{0,i}(x) := \sum_{k=0}^{N}\check{v}_{0,i}^k\frac{x^{2k}}{(2k)!} \tag{31}$$

and

$$\check{v}_{T,i}(x) := \sum_{k=0}^{N}\check{v}_{T,i}^k\frac{x^{2k}}{(2k)!}, \tag{32}$$

for $N \in \mathbb{N}$ and $\check{v}_{0,i}^k, \check{v}_{T,i}^k \in \mathbb{R}$, since the algebra of even polynomials on $x \in [0,1]$ separates points and is dense in $C([0,1])$, and hence $\mathcal{L}^2(0,1)$. In particular, for any $\delta > 0$, there exists $N \in \mathbb{N}$ large enough such that

$$\|\check{v}_{T,i}(\cdot) - v_{T,i}(\cdot)\|_{\mathcal{L}^2(0,1)} < \delta. \tag{33}$$

We now generate the open–loop controller (30) to transition from (31) to (32), which we accomplish through design of suitable $y_i(t)$. As in Laroche et al. [2000], we select

$$y_i(t) = \left(1 - \Phi_\gamma(t-t_0)\right)\sum_{k=0}^{N}\varepsilon_i^k\check{v}_{0,i}^k\frac{(t-t_0)^k}{k!} + \Phi_\gamma(t-t_0)\sum_{k=0}^{N}\varepsilon_i^k\check{v}_{T,i}^k\frac{(t-t_0-T)^k}{k!}, \tag{34}$$

for $\varphi(t) := \begin{cases} 0 & t = 0,\, T \\ e^{-\frac{1}{(t(T-t))^{\gamma}}} & t \in (0,T) \end{cases}$, and

$$\Phi_{\gamma}(t) := \frac{\int_0^t \varphi_{\gamma}(\tau) d\tau}{\int_0^T \varphi_{\gamma}(\tau) d\tau}, \quad T \in [0,T] \tag{35}$$

where $\gamma \in \mathbb{R}_{>1}$, which ensures that $y_i^{(k)}(t_0) = \varepsilon_i^k \check{v}_{0,i}^k$, $y_i^{(k)}(t_0 + T) = \varepsilon_i^k \check{v}_{T,i}^k$, for $k = 0, \ldots, N$, with subsequent derivatives equal to zero. Moreover, the selection (34) ensures the necessary Gevrey class regularity of $y_i(t)$ and that the output trajectory smoothly transitions between its initial and final states. Depending on the initial and terminal profiles selected, (34) can be designed as a smooth ramping function, which is desirable, for example, in chemical reactor processes where one is often tasked with *ramping* concentrations of reagents during start–up, shutdown and operating point transitioning processes. Different output trajectories satisfying the necessary Gevrey class regularity can also be designed; in this work, we specialize to the one selected in (34). In order to implement (30) in practice, we can uniformly approximate the infinite sum with its first M terms, for $M \in \mathbb{N}$ sufficiently large, under which (33) still holds. The treatment for different v_j, $j \neq i$, is equivalent.

Hence, given initial conditions $v_0(x) \in \mathcal{L}^2(0,1)^n$ and desired terminal conditions $v_T(x) \in \mathcal{L}^2(0,1)^n$, the above treatment allows one to generate the open–loop controller (30), for $i = 1, \ldots, n$, which approximately transitions from $v_0(x)$ to $v_T(x)$. Moreover, since (11) is the identity operator at $x = 0$, this controller assigns a *smooth* output trajectory from $\check{v}_0(0)$ to $\check{v}_T(0)$. To design $U_{\mathrm{T}}(t)$ such that it steers $u_0(x) \in \mathcal{L}^2(0,1)^n$ to a desired $u_T(x) \in \mathcal{L}^2(0,1)^n$, one need only transform these profiles for the plant into ones for the target system (14)–(16) by using (11). Next, we enhance our control law to allow for different initial conditions.

3.3 Prescribed–time trajectory tracking

The open–loop controller developed in Section 3.2 is only valid for a single initial condition for the plant, given by transforming (31) for $i = 1, \ldots, n$ by (12). For different initial conditions $u_0 \in \mathcal{L}^2(0,1)^n$, one would like to track the desired output trajectory and maintain the transition to $u_T(x)$. With these goals in mind, we henceforth refer to (29) (generated by (34) and hence (30)) as the *reference state* and denote it by $v_{\mathrm{ref}}(x,t)$ (with associated plant reference state $u_{\mathrm{ref}}(x,t)$).

To track the desired output trajectory, we introduce error feedback which corrects error in U_{T} due to different initial conditions. We define

$$e(x,t) := v(x,t) - v_{\mathrm{ref}}(x,t). \tag{36}$$

Particular to our treatment is the rate of attractivity of the error to the origin: we wish to achieve $e(x,t) \to 0$ as $t \to t_0 + T$, for any $0 < T < \infty$. Immediate ramifications are maintaining the transition from *any* $v_0(x)$ to the desired $\check{v}_T(x)$ and prescribed–time output trajectory tracking.

Notice from (14)–(16) and (25)–(27) that $e(x,t)$ satisfies

$$\frac{\partial e}{\partial t}(x,t) = \Sigma \frac{\partial^2 e}{\partial x^2}(x,t), \tag{37}$$

$$\frac{\partial e}{\partial x}(0,t) = 0, \tag{38}$$

$$e(1,t) = U_{\mathrm{PT}}(t), \tag{39}$$

with initial condition $e_0(x) = v_0(x) - \check{v}_0(x) \not\equiv 0$ in general; this system is already stable albeit at an exponential rate stipulated by Σ. To achieve a faster stabilization rate, we follow the time–varying feedback treatment in Steeves et al. [2019]: we define the linear function

$$\nu(t - t_0) := 1 - \frac{t - t_0}{T} \tag{40}$$

and its corresponding "blow–up" function

$$\mu_3(t - t_0) := \frac{1}{\nu^3(t - t_0)}. \tag{41}$$

We have the following stabilization result concerning (37)–(39).

Lemma 4. Selecting

$$U_{\mathrm{PT},i}(t) = \int_0^1 K_{\mathrm{PT},i}(1,y,t-t_0) e_i(y,t) dy \tag{42}$$

for $i = 1, \ldots, n$, with

$$K_{\mathrm{PT},i}(x,y,t-t_0) = -\frac{\mu_{0,i}}{2\varepsilon_i \nu^3(t-t_0)} \sum_{l=0}^{\infty} \frac{\left(\frac{x^2 - y^2}{4\varepsilon_i T \nu(t-t_0)}\right)^l}{(l+1)!} \times \sum_{j=0}^{l} \sum_{k=0}^{j} \binom{j}{k} \binom{l+2+k}{l-j} \frac{\left(\frac{\mu_{0,i} T}{2\nu^2(t-t_0)}\right)^j}{j!}, \tag{43}$$

which is smooth in $\mathcal{T} \times [t_0, t_0 + T)$, and

$$\mu_{0,i} > \frac{4}{\varepsilon_i T^3} \tag{44}$$

yields

$$\|e(\cdot,t)\|_{\mathcal{L}^2(0,1)^n} \leq C e^{-\frac{rT}{2\nu^2(t-t_0)}} \|e_0(\cdot)\|_{\mathcal{L}^2(0,1)^n} \to 0 \tag{45}$$

as $t \to t_0 + T$, for $C > 0$ and $r = \min_{1 \leq i \leq n} \{\mu_{0,i} - \frac{2\sqrt{\mu_{0,i}}}{\sqrt{\varepsilon_i} T^{3/2}}\} > 0$. Moreover, $U_{\mathrm{PT}}(t)$ remains bounded for all $t \in [t_0, t_0 + T)$, and $U_{\mathrm{PT}}(t) \to 0$ as $t \to t_0 + T$.

The design of (42)–(44) utilizes the backstepping method and a time–varying damping technique to ensure the desired prescribed–time stabilization of the error. For a proof of Lemma 4, see Steeves et al. [2019]. We are now in the position to prove our main theorem.

3.4 Proof of Theorem 1

First, notice from (36) and (42) that $U_{\mathrm{PT}}(t)$ is in feedback form for the target system (14)–(16). To render $U_{\mathrm{PT}}(t)$ into feedback form for the plant, we rely on the backstepping transformation (11), which appears in the second line of the control law (8).

Lemma 4 establishes the state transition from $v_0(x)$ to $\check{v}_T(x)$ (which uniformly approximates the desired terminal profile for target system (14)–(16)) within the terminal time. Due to (17), it follows from (45) that the desired approximate state transition is still achieved by the terminal time for the plant. To design the desired state transition for the plant, one selects a feasible initial condition and a desired terminal profile, and then maps these to the target system states via (11). The ensuing open–loop control component is designed using these functions.

The control gains appearing in (8) are smooth in time and continuous in $\mathcal{T}$, as stated in Lemmas 2 and 4. Due to (17) and Lemma 4, the feedback controller remains bounded provided that the state remain bounded for $t \in [t_0, t_0 + T)$; the latter property is ensured in the subsequent section.

Since (11) is nothing but the identity operator at $x = 0$ and by (7), it follows that the output trajectory for the closed–loop system tracks (34) with zero error by the terminal time.

Well–posedness of the closed–loop system up until the terminal time can be verified by first studying well–posedness of the target system and then relaying this result back to the plant by using the associated inverse transformations.

4. SIMULATIONS

We simulate our prescribed–time approximate state transitioning and output trajectory tracking control law for a system of two equations, given by

$$\frac{\partial u_1}{\partial t} = \varepsilon_1 \frac{\partial^2 u_1}{\partial x^2} + \lambda_{11} u_1 + \lambda_{12} u_2, \tag{46}$$

$$\frac{\partial u_2}{\partial t} = \varepsilon_2 \frac{\partial^2 u_2}{\partial x^2} + \lambda_{22} u_2, \tag{47}$$

$$\frac{\partial u_1}{\partial x}(0,t) = 0, \ \frac{\partial u_2}{\partial x}(0,t) = 0, \tag{48}$$

$$u_1(1,t) = U_1(t), \ u_2(1,t) = U_2(t), \tag{49}$$

for $\varepsilon_1 = 2$, $\varepsilon_2 = 1.5$, $\lambda_{11} = \pi$, $\lambda_{21} = -2$, $\lambda_{22} = 2\pi$, and the control law developed above with $\gamma = 1.9$ and $\mu_{0,1} = \mu_{0,2} = 4$. We prescribe the terminal time $T = 2$.

In our first simulation, we wish to achieve a smooth ramping for the output trajectories, which is desirable in start–up, shut-down and operating point transitioning processes. We assign the nominal initial conditions $v_0(x) = [0 \quad 0]^T$ and terminal profiles $u_T(x) = \left[T_D^{-1}[1] \quad T_D^{-1}[0.5]\right]$ used in generating the approximate controller (30) with $N = 2$ and $M = 4$, which produces the desired smooth output ramping due to (34). We select $u_0(x) = [5x \quad 3 - 3x^3]^T$ as the plant's true initial conditions. Figure 1 demonstrates the outputs of (46)–(49) converging to the desired output trajectories; moreover, Figure 2 shows the error due to variation in nominal/true initial conditions attenuating to zero at the rate (45) (evidently faster than exponential decay).

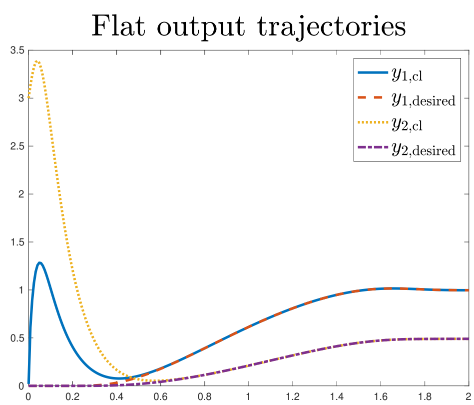

Fig. 1. Simulation 1: prescribed–time output trajectory tracking for (46)–(49) for specified ramping trajectories.

In our second simulation, we wish to achieve approximate state transitioning to desired terminal profiles. We again assign the nominal initial conditions $v_0(x) = [0 \quad 0]^T$ and select terminal profiles $u_T(x) = \left[x^3 \quad 0.5\right]$ for generating (30). The cubic terminal profile is selected to demonstrate that our approach of approximating by even polynomials in (32) is not limiting. Moreover, these terminal profiles are markedly not stationary for (46)–(49). We select $u_0(x) = [10x^2 \quad 2 - 2x^3]^T$ as the plant's true initial conditions. Figures 3 and 4 demonstrate the approximate state transitioning, while Figure 5 shows initial condition error attenuation and displays surface plots of the states with

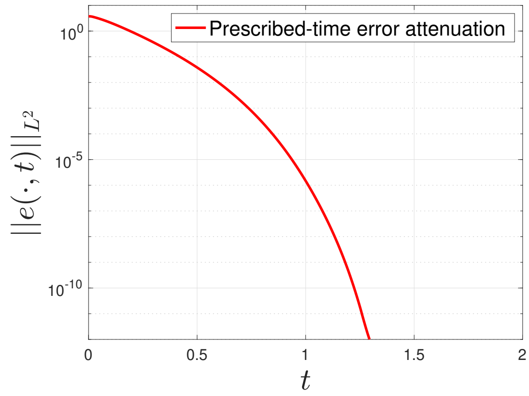

Fig. 2. Simulation 1: prescribed–time error attenuation for (37)–(39).

the boundary inputs indicated. The error in achieving $u_{T,2}$ in Figure 3 is mainly accounted for by (32), whereas the error displayed in Figure 4 is due to the approximations of K_D, K_PT and U_T.

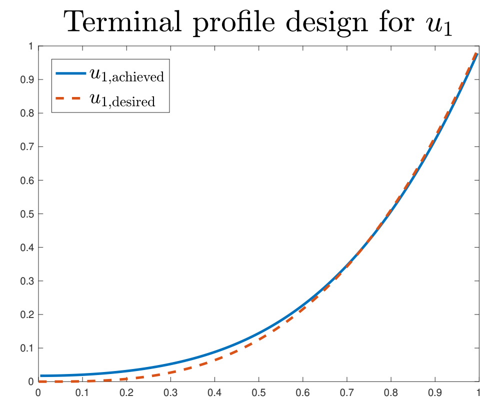

Fig. 3. Simulation 2: approximate state transitioning for (46).

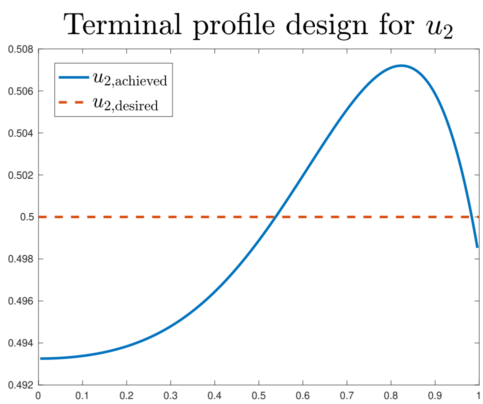

Fig. 4. Simulation 2: approximate state transitioning for (47).

These simulations were carried out using the implicit Euler method. The control gain K_D is approximated using the power series method described in Camacho-Solorio et al. [2017] with degree eight, whereas K_PT is given explicitly in (43) and approximated by the first ten terms. Hence, these control gains

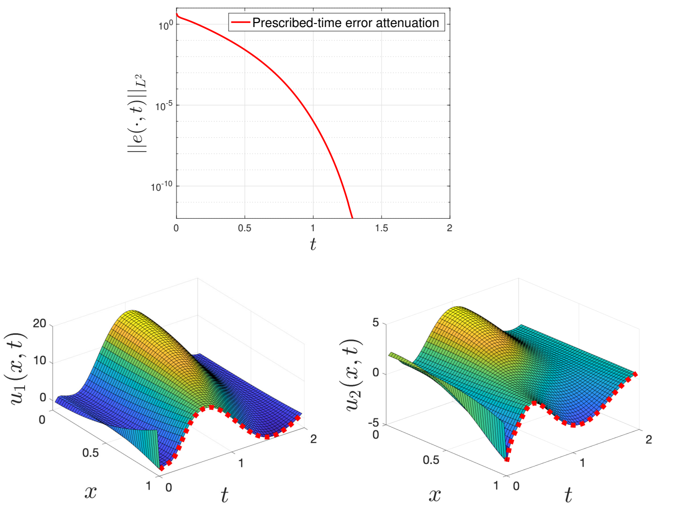

Fig. 5. Simulation 2: approximate state transitioning for (46)–(47), with prescribed–time error attenuation. Boundary control laws appear as dotted red lines.

can be readily pre–calculated given the system parameters. In contrast, the open–loop controller (30) requires computationally expensive symbolic calculations for every set of initial conditions and terminal profiles. This motivates our use of error feedback for implementation purposes, ensuring finite–time error attenuation to zero independently of (the size of) initial conditions.

While one can aim approximate any terminal profiles for (46)–(49), this comes at the cost of requiring large N and hence usually large $\check{v}^k_{\mathrm{T},i}$ in (32), leading to very large open–loop controllers which may not be feasible in practice.

5. CONCLUSION

We developed a feedback control law which performs approximate state transitioning and prescribed–time output trajectory tracking. The control law proposed herein drives the closed–loop system (1)–(6) from *any* $\mathcal{L}^2$ initial conditions to stationary *or* non–stationary terminal profiles which uniformly approximate desired ones. Alternatively, the controllers can be designed such that the closed–loop system's output (7) tracks desired smooth reference trajectories (34).

Control laws achieving prescribed–time output trajectory tracking and approximate state transitioning *which depend only on the output* are of interest because they allow for *uncertain* initial conditions. This extension is left as a future work.

REFERENCES

Farid Ammar-Khodja, Assia Benabdallah, Manuel González Burgos, and Luz de Teresa. Recent results on the controllability of linear coupled parabolic problems: a survey. *Mathematical Control and Related Fields*, 1(3): 267–306, 2011.

Antonello Baccoli, Alessandro Pisano, and Yury Orlov. Boundary control of coupled reaction–diffusion processes with constant parameters. *Automatica*, 54:80–90, 2015.

Leobardo Camacho-Solorio, Rafael Vazquez, and Miroslav Krstic. Boundary observer design for coupled reaction-diffusion systems with spatially-varying reaction. In *2017 American Control Conference (ACC)*, pages 3159–3164. IEEE, 2017.

Jean-Michel Coron. *Control and nonlinearity*. Number 136. American Mathematical Soc., 2007.

Jean-Michel Coron and Hoai-Minh Nguyen. Null controllability and finite time stabilization for the heat equations with variable coefficients in space in one dimension via backstepping approach. *Archive for Rational Mechanics and Analysis*, 225(3):993–1023, 2017.

Nicolás Espitia, Andrey Polyakov, Denis Efimov, and Wilfrid Perruquetti. Boundary time–varying feedbacks for fixed-time stabilization of constant-parameter reaction–diffusion systems. *Automatica*, 103:398–407, 2019.

Hector O Fattorini. Control in finite time of differential equations in banach space. *Communications on Pure and Applied Mathematics*, 19(1):17–34, 1966.

Hector O Fattorini and David L Russell. Exact controllability theorems for linear parabolic equations in one space dimension. *Archive for Rational Mechanics and Analysis*, 43(4): 272–292, 1971.

Michel Fliess, Jean Lévine, Philippe Martin, and Pierre Rouchon. Flatness and defect of non-linear systems: introductory theory and examples. *International journal of control*, 61(6): 1327–1361, 1995.

Gerald B Folland. *Introduction to partial differential equations*. Princeton university press, 1995.

Andrei V Fursikov and Oleg Yu Imanuvilov. On controllability of certain systems simulating a fluid flow. In *Flow Control*, pages 149–184. Springer, 1995.

Maurice Gevrey. Sur la nature analytique des solutions des équations aux dérivées partielles. premier mémoire. In *Annales Scientifiques de l'Ecole Normale Supérieure*, volume 35, pages 129–190, 1918.

Alan Hastings. Global stability in lotka-volterra systems with diffusion. *Journal of Mathematical Biology*, 6(2):163–168, 1978.

Miroslav Krstic and Andrey Smyshlyaev. *Boundary control of PDEs: A course on backstepping designs*, volume 16. SIAM, 2008.

Béatrice Laroche, Philippe Martin, and Pierre Rouchon. Motion planning for the heat equation. *International Journal of Robust and Nonlinear Control: IFAC-Affiliated Journal*, 10 (8):629–643, 2000.

Philippe Martin, Lionel Rosier, and Pierre Rouchon. Null controllability of the heat equation using flatness. *Automatica*, 50(12):3067–3076, 2014.

Thomas Meurer. *Control of Higher–Dimensional PDEs: Flatness and Backstepping Designs*. Springer Science & Business Media, 2012.

Andrey Polyakov, Denis Efimov, and Wilfrid Perruquetti. Finite-time and fixed-time stabilization: Implicit lyapunov function approach. *Automatica*, 51:332–340, 2015.

Walter Rudin et al. *Principles of mathematical analysis*, volume 3. McGraw-hill New York, 1964.

Drew Steeves, Miroslav Krstic, and Rafael Vazquez. Prescribed–time stabilization of reaction–diffusion equations by output feedback. In *Proceeding of the American Control Conference (ACC)*, pages 2570–2575. IEEE, 2019.

Rafael Vazquez and Miroslav Krstic. Boundary control of coupled reaction-advection-diffusion systems with spatially-varying coefficients. *IEEE Transactions on Automatic Control*, 62(4):2026–2033, 2017.

Joseph J Winkin, Denis Dochain, and Philippe Ligarius. Dynamical analysis of distributed parameter tubular reactors. *Automatica*, 36(3):349–361, 2000.